SvedbergOpen
DISSEMINATION OF KNOWLEDGE

International Journal of Artificial Intelligence and Machine Learning

Publisher's Home Page: https://www.svedbergopen.com/

Research Paper Open Access

Ranking-Based performance Analysis of Hierarchical Computing Network under Task Impatience

Sachin R. Gurnule[1], P. Pranay[2], V.N. Rama Devi[3], Mallika Dhingra[4]

[1]Research Scholar, Department of Mathematics and Statistics, Chaitanya (Deemed to be University), Warangal, Telangana, sgurnule28@gmail.com
[2]Associate Professor, Department of Mathematics and Statistics, Chaitanya (Deemed to be university), Telangana, pettempranay@gmail.com
[3]Professor, Department of Statistics, Gokaraju Rangaraju Institute of Engineering and Technology, Hyderabad, ramadevivn@gmail.com
[4]Founder & Director of Research, Perpetua Education and Research Solutions, Gurugram, Haryana, India,
Email: mallikadhingra13@gmail.com
Corresponding Author: Dr. V.N. Rama Devi, Professor, Department of Statistics, GRIET, Hyderabad, ramadevivn@gmail.com

Abstract
Computer networks and distributed processing systems often operate under uncertain traffic conditions, where arrival rates, service rates and task abandonment cannot be represented precisely by crisp parameters. This study presents a ranking-based performance analysis of an M/M/1 Jackson-type network queueing system with task impatience under fuzzy and intuitionistic fuzzy environments. The proposed model consists of two processing nodes and one Central Server with finite capacity, external arrivals, routing from nodes to the Central Server, balking and reneging. Triangular fuzzy, trapezoidal fuzzy, triangular intuitionistic fuzzy and trapezoidal intuitionistic fuzzy numbers are used to represent uncertain arrival and service rates. The transient state probabilities are formulated through Kolmogorov forward equations and solved numerically using the fourth-order Runge–Kutta method in MATLAB. Expected system length and mean waiting time are evaluated for Node-1, Node-2 and the Central Server. Robust ranking and wingspan methods are applied to convert fuzzy and intuitionistic fuzzy performance measures into comparable ranked values. The results show that uncertainty decreases as the α-cut value increases in fuzzy models, while β-cut based intuitionistic fuzzy models provide more compact and stable intervals. Trapezoidal fuzzy and trapezoidal intuitionistic fuzzy models give more controlled uncertainty ranges than triangular fuzzy models. Node-1 shows the lowest congestion, Node-2 shows moderate congestion and the Central Server shows the highest congestion. The proposed approach is useful for congestion-aware task scheduling, routing control and capacity planning in computer networks, cloud systems and distributed computing environments.

Keyword: Jackson network, Central Server, task impatience, fuzzy queueing, intuitionistic fuzzy set, robust ranking, wingspan method.

Introduction

Computer networks, cloud computing platforms, distributed processing systems and data communication infrastructures are increasingly required to handle large volumes of heterogeneous tasks, packets and service requests. In such systems, incoming jobs may pass through several processing units such as edge nodes, routers, gateways, servers, data centres or central processing units before completion. The performance of these systems is mainly affected by traffic intensity, service capacity, routing probability, waiting time, congestion and task abandonment. Therefore, queueing theory provides an important mathematical framework for analysing delay, buffer occupancy and resource utilization in computer and communication systems [1,2,7-13].

Jackson network queueing models are widely used to represent interconnected service systems in which jobs move from one service node to another according to specified routing probabilities. In the context of computer science engineering, such models can be used to represent packet-switched networks, cloud task scheduling systems, distributed server architectures, database transaction systems and multi-stage processing networks. The M/M/1 Jackson-type network is particularly useful when each processing node is modelled as a single-server queue with Poisson arrivals and exponentially distributed service times. Jackson's classical network model provides a strong theoretical basis for analysing open queueing networks and their performance measures [3-6,10-13].

However, in real computer networks, arrival rates and service rates are rarely fixed or exactly known. Network traffic may fluctuate due to user demand, packet burstiness, server load variation, routing changes, hardware limitations and congestion. Similarly, service rates may vary because of processor speed, memory availability, bandwidth allocation, scheduling policy and system failure. In such an uncertain environment, classical queueing models with crisp parameters may be inadequate to describe realistically the behaviour of the system. In order to overcome this limitation, using fuzzy set theory introduced by Zadeh, imprecise arrival and service parameters are represented by triangular and trapezoidal fuzzy numbers, respectively [14-16,18-21]. Moreover, intuitionistic fuzzy set theory has the ability to model membership degrees, non-membership degrees and hesitation degrees, which is helpful when uncertainty is not only due to the imprecision, but also due to incomplete information and hesitant information [17,25].

Task impatience is another important practical issue in computer networks. Excessive delay, timeout, dropping of packets, buffer overflow, expiry of sessions or user cancel may cause a task or packet or userrequest to leave the system without being served. Balking and reneging mechanisms can be used to model such behaviour. Reneging is defined as an exiting task not completing the task because of delay and balking is defined as an arriving task not joining the queue because of congestion. Customer or task impatience leads to a more realistic queueing model for modern computer systems, which have to serve delay-sensitive tasks such as video streaming, online transactions, cloud service and real-time communication [7-13,18-21].

In fuzzy and intuitionistic fuzzy queueing models, the system performance measures like expected system length, mean waiting time etc., are typically in interval or in fuzzy form. It is hard to compare these values one by one, particularly if the fuzzy intervals overlap. Hence, ranking methods are needed to defuzzify fuzzy, and intuitionistic fuzzy, performance measures to obtain a comparable crisp index. This can be accomplished by using the robust ranking and wingspan methods which take into account both the central tendency and the spread of fuzzy quantities. These ranking methods can be used to detect congested nodes, to compare their delay behaviour and to make decisions in the presence of uncertain network conditions [22-25].

The present study focuses on a ranking-based performance analysis of an M/M/1 Jackson-type computer network queueing system with task impatience under fuzzy and intuitionistic fuzzy environments. The system consists of two processing nodes and one Central Server or central server. Tasks may arrive externally at each node, receive service, and may be routed from the individual nodes to the central server. The model also incorporates balking and reneging to represent task abandonment. Triangular fuzzy, trapezoidal fuzzy, triangular intuitionistic fuzzy and trapezoidal intuitionistic fuzzy parameters are considered for arrival and service rates. The α-cut and β-cut approaches are used to examine uncertainty in the performance measures, while robust ranking and wingspan methods are applied to obtain comparable ranked values [14-25].

The main objective of this study is to evaluate expected system length and mean waiting time at Node-1, Node-2 and the central server under uncertain traffic and service conditions. The proposed approach helps to identify the most congested component of the computer network and provides a meaningful comparison of different fuzzy and intuitionistic fuzzy environments, also this study lies in developing a ranking-based performance evaluation framework for a finite-capacity Jackson-type computer network with task impatience under fuzzy and intuitionistic fuzzy environments. Unlike classical crisp queueing models, the proposed approach incorporates uncertain arrival and service rates using triangular, trapezoidal and intuitionistic fuzzy parameters, and converts the resulting fuzzy performance measures into comparable ranked values using robust ranking and wingspan methods. [7-13,18-25].

Materials and Method

Queueing Network Model

We considered the Transient Analysis of Jackson type Network Queue consists of two nodes and one Central Server with Task Abandonment as detailed below:

1. The capacity of each node as well as Central Server are assumed as S(finite)
2. The Task Scheduling is allowed from nodes to the Central Server whereas flow from one node to another node is restricted. Also assumed that task can directly enter in to Central server queue. The mean arrival rates at node-1, node-2 and Central server are assumed to follow Poisson Process with respective mean arrival rates λ_1, λ_2 and λ_3.
3. The mean service rates for first essential services at node-1, node-2 and Central Server are μ_1, μ_2 and μ_3.
4. Task at nodes who want additional service from Central Server can opt with optional probabilities of p_1 and p_2 respectivelyss.

5. Task Abandonment is characterized by two sets of parameters: the balking parameters
6. (1-b1), (1-b2) and (1-b3) representing the probabilities that a customer declines to join the queues of node-1, node-2 and Central server; and the reneging parameters ξ_1,ξ_2 and ξ_3, representing the rate at which task abandon the respective queues after waiting.

With the above assumptions and parameter definitions, an infinitesimal generator matrix Q is obtained from derived Kolmogorov forward equations (In order to describe how the state probabilities evolve over time given in appendix.) as follows:

Infinitesimal Generator Matrix Q Formulation

Let

$$X(t)=\{N_1(t),N_2(t),N_3(t)\}$$

denote the state of the system at time t, where N1(t), N2(t), and N3(t) represent the number of tasks at Node-1, Node-2, and the Central Server, respectively. Since the capacity of each service station is finite,

$$0\le N_1,N_2,N_3\le S.$$

The state space of the system is defined as

$$\Omega=\{(i,j,k):0\le i,j,k\le S\}$$

with cardinality

$$|\Omega|=(S+1)^3.$$

Define

$$P(t)=[P_{(I,j,k)}(t)]_{((I,j,k)\in\Omega)}.$$

denote the transient probability vector of the system. Then, the transient behaviour of the system is governed by the Kolmogorov forward equation

$$\frac{dP(t)}{dt}=P(t)Q$$

where

$$Q=[q_{((I,j,k),(r,s,l))}]$$

is an $(S+1)^3\times(S+1)^3$ infinitesimal generator matrix.

(a) Structure of Q

The generator matrix Q has a block tridiagonal structure with respect to the Central Server population level k, and can be written as

$$Q=\begin{bmatrix} D_0 & A_0 & 0 & 0 & \cdots & 0 \\ B_1 & D_1 & A_1 & 0 & \cdots & 0 \\ 0 & B_2 & D_2 & A_2 & \cdots & 0 \\ \vdots & \vdots & \vdots & \vdots & \ddots & \vdots \\ 0 & 0 & 0 & B_S & D_S & \end{bmatrix}$$

where each block is of dimension

$$(S+1)^2\times(S+1)^2.$$

Here

- A_k: transitions increasing the Central Server population (k→k+1)
- B_k: transitions decreasing the Central Server population (k→k-1)
- D_k: transitions within the same Central Server level k

(b)Generic Matrix Elements

For any state (i, j, k) ∈ Ω, the non-zero off-diagonal elements of Q are defined as follows.

External Arrivals

$$q_{((i,j,k),(i+1,j,k))}=\lambda_1 b_{1},i<S$$
$$q_{((i,j,k),(i,j+1,k))}=\lambda_2 b_{2},j<S$$
$$q_{((i,j,k),(i,j,k+1))}=\lambda_3 b_{3},k<S$$

Service Completions and Reneging at Node-1

For $i \geq 1$, a task may leave Node-1 after service completion without routing to the Central server. In addition, if $i \geq 2$, waiting tasks may abandon the queue due to reneging.

Therefore,

$$q_{((i,j,k),(i-1,j,k))}=(1-p_1)\mu_1+(i-1)\xi_1,i \geq 1$$

When i = 1, the reneging term becomes zero.

Service Completions and Reneging at Node-2

Similarly, for Node-2,

$$q_{((i,j,k),(i,j-1,k))}=(1-p_2)\mu_2+(j-1)\xi_2,j \geq 1$$

When j = 1, the reneging term becomes zero.

Service Completions and Reneging at the Central Server

For the Central Server,

$$q_{((i,j,k),(i,j,k-1))}=\mu_3+(k-1)\xi_3,k \geq 1$$

When k = 1, the reneging term becomes zero.

Routing from Nodes to the Central Server

After service completion at Node-1, a task may be routed to the Central Server with probability p1.
Therefore,

$$q_{((i,j,k),(i-1,j,k+1))}=p_1 \mu_1,i \geq 1,k < S.$$

Similarly, after service completion at Node-2, a task may be routed to the Central Server with probability p2. Therefore,

$$q_{((i,j,k),(i,j-1,k+1))}=p_2 \mu_2,j \geq 1,k < S.$$

Diagonal Elements

The diagonal elements of the infinitesimal generator matrix are defined as the negative sum of all transition rates out of the state (i, j, k). Thus,

$$q_{(i,j,k),(i,j,k)} = -\sum_{(r,s,l)\neq(i,j,k)} q_{(i,j,k),(r,s,l)}.$$

All other elements of Q are zero. This construction ensures that each row of the generator matrix sums to zero, which is required for a valid continuous-time Markov chain representation of the finite-capacity queueing network.

The Robust Ranking method and Wingspan method are detailed here with:

Using the robust ranking method, the fuzzy numbers or intuitionistic fuzzy numbers are converted into a single scalar value and the uncertainty information is preserved. It is particularly valuable in queueing models (such as Jackson networks) for comparably assessing the performance of systems.

Robust Ranking for Fuzzy Numbers (Triangular / Trapezoidal)

For a triangular fuzzy number

$$\tilde{A} = (a_1, a_2, a_3)$$

The robust ranking index is:

$$R(\tilde{A}) = \frac{a_1 + a_2 + a_3}{3} + \frac{a_3 - a_1}{6}$$

or a trapezoidal fuzzy number

$$\tilde{A} = (a_1, a_2, a_3, a_4)$$
$$R(\tilde{A}) = \frac{a_1 + a_2 + a_3 + a_4}{4} + \frac{(a_4 - a_1) + (a_3 - a_2)}{6}$$

Robust Ranking for Intuitionistic Fuzzy Numbers (IFM)

An IFM is

$$\tilde{A} = (\mu, \nu)$$

where

- μ→ membership
- ν→ non-membership
- hesitation = 1-μ-ν

Robust ranking:

$$R(\tilde{A}) = \mu - \nu + \frac{1 - \mu - \nu}{2}$$

from the lower and upper bounds of α-cuts and β-cuts:

$$R = \frac{L + U}{2} + \frac{U - L}{6}$$

where

- L= lower bound
- U= upper bound

Wingspan Method (Triangular and Trapezoidal)

The wingspan method is a ranking technique used to compare fuzzy and intuitionistic fuzzy numbers by considering both the central value and the spread (uncertainty width). It emphasizes how "wide" the fuzzy number is, hence the name wingspan.

Wingspan = Right spread + Left spread

This method ranks fuzzy numbers by combining both.

For Triangular Fuzzy Number

Let $\tilde{A} = (a_1, a_2, a_3)$

Center (C)	Wingspan (W)	Ranking index
$C = \frac{a_1 + a_2 + a_3}{3}$	$W = a_3 - a_1$	$R(\tilde{A}) = C + \frac{W}{2}$

For Trapezoidal Fuzzy Number

Let $\tilde{A} = (a_1, a_2, a_3, a_4)$

Center (C)	Wingspan (W)	Ranking index
$C = \frac{a_1 + a_2 + a_3 + a_4}{4}$	$W = (a_4 - a_1)$	$W = (a_4 - a_1)$

For Interval (α-cut / β-cut values)

For the bounds of $[L, U]$

Center (C)	Wingspan (W)	Ranking index
$C = \frac{L + U}{2}$	$W = U - L$	$R = \frac{L + U}{2} + \frac{U - L}{2} = U$

Wingspan method leans toward upper bound.

For Intuitionistic Fuzzy (IFM)

For IFM:

- Membership → μ
- Non-membership → ν

Wingspan idea:

- Spread = hesitation = 1-μ-ν

Performance Measures

1. Expected lengths of the Node-1, Node-2 and Central Server (L_N1^((t)),L_N2^((t)) and L_HO^((t))) where,

$L_{N1}^{(t)}$	$L_{N2}^{(t)}$	$L_{HO}^{(t)}$
$L_{N1}^{(t)} = \sum_{i=0}^{s}\sum_{j=0}^{s}\sum_{k=0}^{s} ip_{i,j,k}^{(t)}$	$L_{N2}^{(t)} = \sum_{i=0}^{s}\sum_{j=0}^{s}\sum_{k=0}^{s} jp_{i,j,k}^{(t)}$	$L_{HO}^{(t)} = \sum_{i=0}^{s}\sum_{j=0}^{s}\sum_{k=0}^{s} kp_{i,j,k}^{(t)}$

2. Mean Processing Delays at Node-1, Node-2 and Central server are represented as ($W_{N1}^{(t)}$, $W_{N2}^{(t)}$ and $W_{HO}^{(t)}$) and are given as

$W_{N1}^{(t)}$	$W_{N2}^{(t)}$	$W_{HO}^{(t)}$)
$W_{N1}^{(t)} = \frac{LN_1(t)}{\lambda_1 b_1}$	$W_{N2}^{(t)} = \frac{LN_2(t)}{\lambda_2 b_2}$	$W_{HO}^{(t)} = \frac{LN_2(t)}{\lambda_3 b_3 + p_1\mu_1 + p_2\mu_2}$

Observation and Results

Since an analytical solution is not tractable for the considered finite-capacity network with routing and impatience, the resulting system of ordinary differential equations is solved numerically using the fourth-order Runge-Kutta (RK4) method in MATLAB. The computed transient probabilities are subsequently used to evaluate the expected queue lengths and mean waiting times. The transient state probabilities were updated by using Runge-Kutta method of order 4 with time step size of 0.5(Δt = 0.5), truncation error of $O(\Delta t^4)$ and convergence tolerance of 10^{-6}.:

The traffic intensities for stability of the model are defined as

Traffic intensities	Formula
$\rho_1(i)$	$\rho_1(i) = \frac{\lambda_1 b_1}{\mu_1 + (i-1) * \xi_1}; 0 \le i \le s$
$\rho_2(j)$	$\rho_2(j) = \frac{\lambda_2 b_2}{\mu_2 + (j-1) * \xi_2}; 0 \le j \le s$
$\rho_3(k)$	$\rho_3(k) = \frac{\lambda_3 b_3 + p_1\mu_1 + p_2\mu_2}{\mu_3 + (k-1) * \xi_3}; 0 \le k \le s$

For these numerical illustrations, the values for all the model parameters are chosen that which satisfy traffic intensity and they are

S=3, λ_1=0.01, λ_2=0.015, λ_3=0.02, μ_1=0.02, μ_2=0.025, μ_3=0.03, ξ_1=0.001, ξ_2=0.0015, ξ_3=0.002, b_1=0.5, b_2=0.55, b_3=0.6, p_1=0.001 and p_2=0.0015.

Table 1 : The Pattern of mean lengths and waiting times of each node and Central Server over different time instances with these metrics are resulted in the following table:

Cons tants	t_1	t_2	t_3	t_4	t_5
$L_{N1}^{(t)}$	0.00000000775 8	0.000000061633	0.000000206563	0.000000486214	0.000000943000
$L_{N2}^{(t)}$	0.00000003472 8	0.000000274957	0.000000918369	0.000002154331	0.000004164127

$L_{HO}^{(t)}$	0.000000106481	0.000000839975	0.000002795294	0.000006533215	0.000012581627
$W_{N1}^{(t)}$	0.000024825781	0.000197226692	0.000661002136	0.001555885038	0.003017600169
$W_{N2}^{(t)}$	0.000067352098	0.000533250923	0.001781080336	0.004178099679	0.008075894209
$W_{HO}^{(t)}$	0.000141974189	0.001119966589	0.003727062786	0.008710972066	0.016775572796

We have studied the model in two scenarios [I & II] to explore various patterns of queue constants, where Scenario-I (Graph: 5.1.1(a), 5.1.1(b) to 5.2.3(a), 5.2.3(b)) shows the behaviour of queue constants over time in Fuzzy in both Robust ranking and Wingspan methods, whereas Scenario- II (5.3.1(a), 5.3.1(b) to 5.4.3(a), 5.4.3(b)) deals with the behaviour of queue constants over time in Intuitionistic Fuzzy model

Triangular Fuzzy Number (Scenario I)

Let us consider an FM/FM/1, Jackson network queueing system with two nodes and one Central Server. Suppose the arrivals rates and service rates are triangular fuzzy numbers and are represented as

α = [0, 0.1, 0.2, 0.3, 0.4, 0.5, 0.6, 0.7, 0.8, 0.9, 1]
λ_x = [0.005 0.01 0.02]; λ_y = [0.01, 0.015, 0.025]; λ_h = [0.015, 0.02, 0.03]
μ_x = [0.015, 0.02, 0.03]; μ_y = [0.02, 0.025, 0.035]; μ_h = [0.025, 0.03 0.04]

For a given range of values of α, λx, λy, λy, µx, µy and µh the expected length of the system at each node and Central server and waiting times at respective areas are shown from Graphs 5.1.1(a), 5.1.1(b) to 5.1.3(a), 5.1.3(b) by keeping values of other parameters fixed.

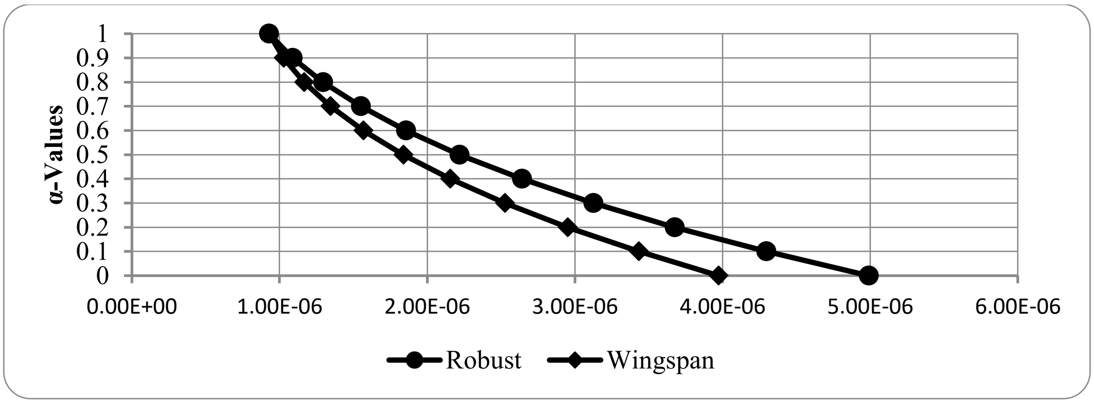

Figure 5.1.1 (a): α-Cut based System Length (LN1) in Robust and Wings span of Triangular fuzzy

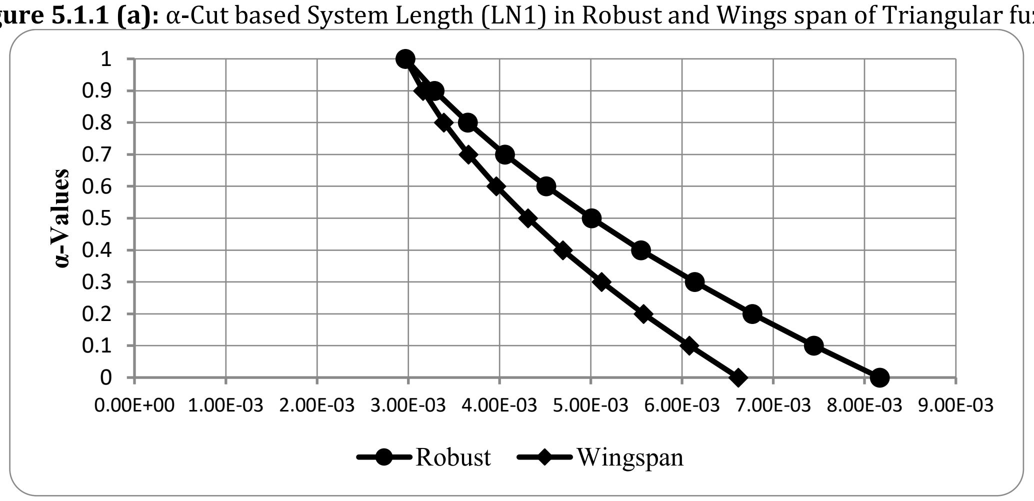

Figure 5.1.1 (b): α-Cut based Waiting Time (WN1) in Robust and Wings span of Triangular fuzzy

From figure 5.1.1(a) and 5.1.1(b) showed α-cut based results for Node-1, it was observed that, expected system length and mean waiting time decrease as the α value increases. This indicates that when the degree of certainty increases, the fuzzy interval becomes narrower and the uncertainty in the queueing performance measures is reduced. The expected system length at Node-1 has a central ranked value of 0.000000943000, which lies within the interval [0.0000009283901726, 0.00000498942345]. Similarly, the mean waiting time has a ranked value of 0.003017600169, lying within the interval [0.00297084947155, 0.00816619462542].

The results suggest that Node-1 experiences a relatively low level of congestion under triangular fuzzy parameters. The difference between the robust ranking and wingspan values reflects the uncertainty associated with the fuzzy arrival and service rates. As α approaches 1, both performance measures move toward more precise values.

Figure 5.1.2(a) : α-Cut based System Length (LN2) in Robust and Wings span of Triangular fuzzy

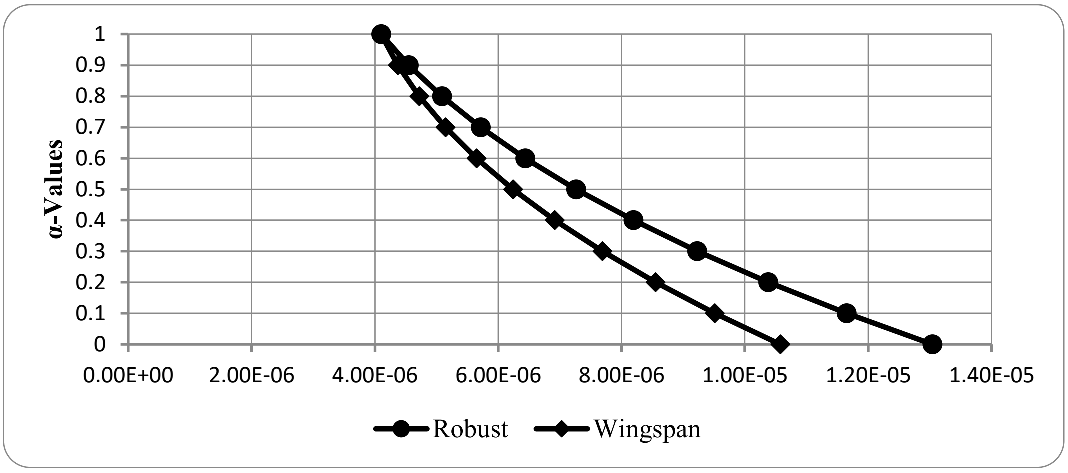

Figure 5.1.2(b) : α-Cut based Waiting Time (WN2) in Robust and Wings span of Triangular fuzzy

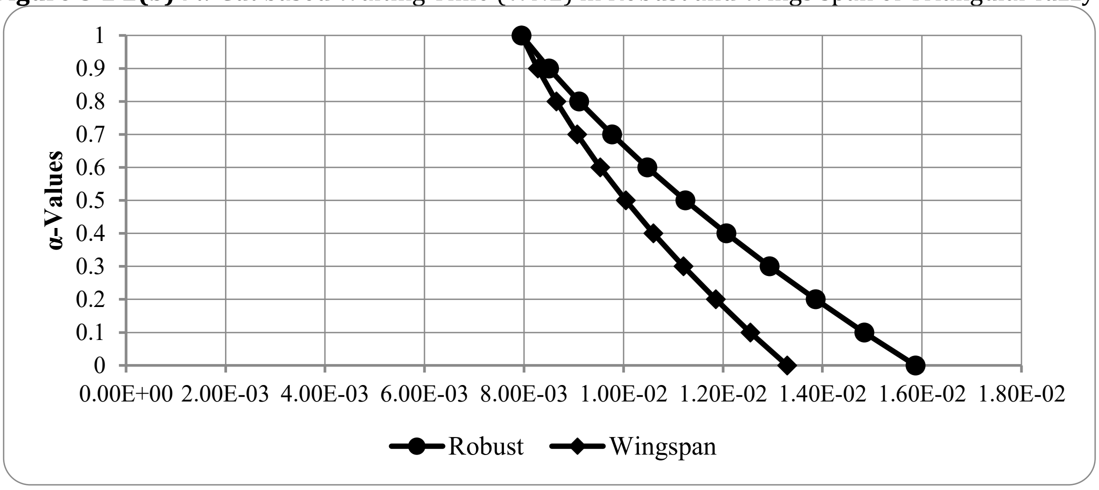

From above graphs 5.1.2(a) and 5.1.2(b) for Node-2, the expected system length and mean waiting time also show a decreasing trend with increasing α values. The expected length has a ranked value of 0.000004164127, which falls within the interval [0.00000409939542, 0.0000105730210384]. The corresponding mean waiting time is 0.008075894209, lying within the interval [0.00795035348841, 0.0132909435482581].

Compared with Node-1, Node-2 shows higher values of both expected system length and waiting time. This indicates that Node-2 is relatively more congested under the assumed fuzzy arrival and service conditions. The reduction in the interval width as α increases confirms that higher confidence levels reduce fuzziness in the estimated performance measures.

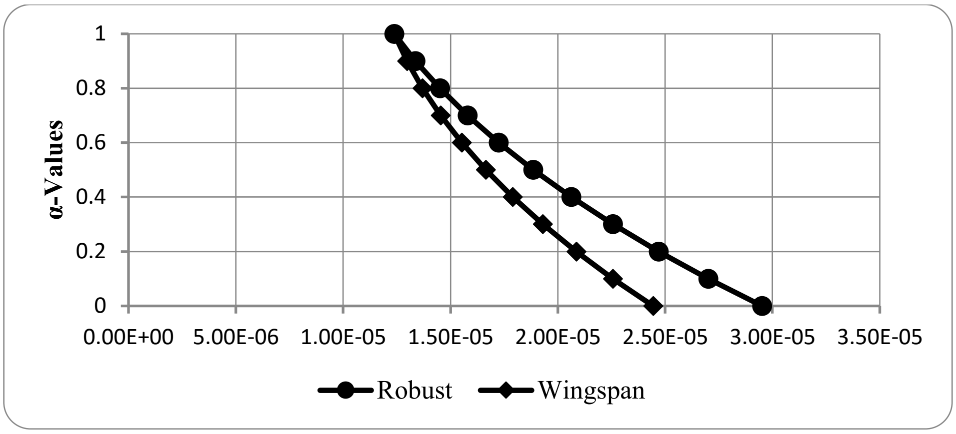

Figure 5.1.3(a) : α-Cut based System Length (LHO) in Robust and Wings span of Triangular fuzzy

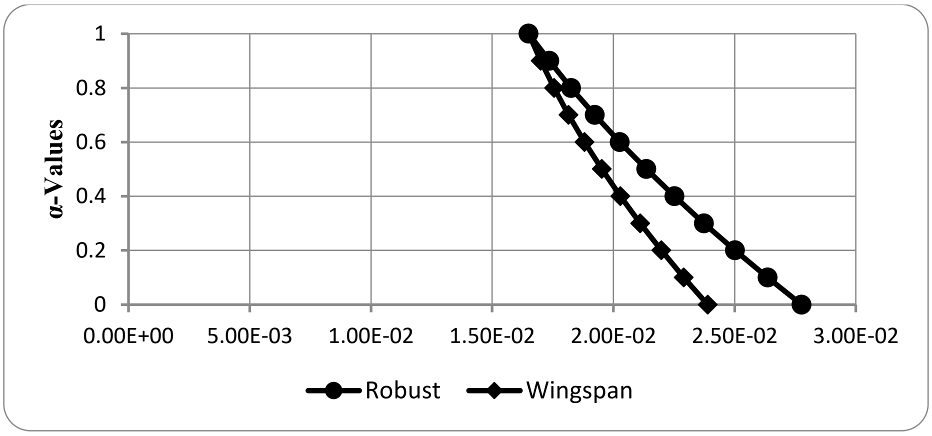

Figure 5.1.3(b) : α-Cut based Waiting Time (WHO) in Robust and Wings span of Triangular fuzzy

From graph 5.1.3(a) and 5.1.3(b) for Central Server shows the highest expected system length and mean waiting time among the three service points. The expected length has a ranked value of 0.000012581627, which lies in the interval [0.00001238109368, 0.00002951621076]. The mean waiting time has a ranked value of 0.016775572796, lying within the interval [0.01650819303224, 0.02776477894694].

This result indicates that the Central Server is the most congested part of the network. The higher values are expected because the Central Server receives direct arrivals as well as routed tasks from Node-1 and Node-2. Therefore, uncertainty in arrival and service rates has a stronger effect at the Central Server than at the individual nodes. The robust ranking and wingspan results show that the Central Server is the most sensitive location in the system and may require higher service capacity or improved routing control.

Triangular Intuitionistic Fuzzy Number

Let us consider an IFM/IFM/1, Jackson network queueing system with two nodes and one Central Server. Suppose the arrivals rates and service rates are triangular Intuitionistic fuzzy numbers and are represented as

Beta(β) = [0, 0.0005, 0.001, 0.0015, 0.002, 0.0025, 0.003, 0.0035, 0.004, 0.0045, 0.005]
λ_x = [0.005 0.01 0.02]; λ_y = [0.01, 0.015, 0.025]; λ_h = [0.015, 0.02, 0.03]
μ_x = [0.015, 0.02, 0.03]; μ_y = [0.02, 0.025, 0.035]; μ_h = [0.025, 0.03 0.04]

For a given range of values of α, λx, λy, λy, μx, μy and μh the expected length of the system at each node and Central Server and waiting times at respective areas are shown from Graphs 5.2.1(a), 5.2.1(b) to 5.2.3(a), 5.2.3(b) by keeping values of other parameters fixed.

Figure 5.2.1 (a) : β-Cut based System Length (LN1) in Robust and Wings span of Triangular Intuitionistic Fuzzy Number

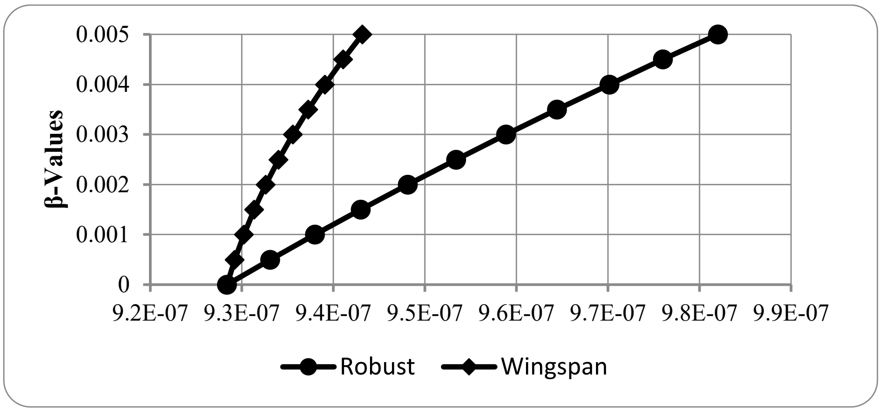

Figure 5.2.1 (b) : β-Cut based Waiting Time (WN1) in Robust and Wings span of Triangular Intuitionistic Fuzzy Number

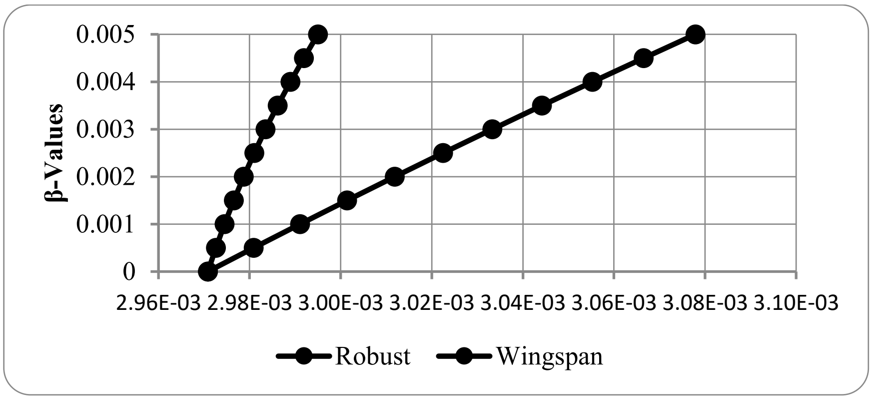

From figure 5.2.1(a) and 5.2.1(b) under the triangular intuitionistic fuzzy environment, the β-cut based results for Node-1 show only a small variation in the expected system length and mean waiting time. The expected length has a ranked value of 0.000000943000 and lies within the interval [0.0000009283901726, 0.0000009820214863]. The mean waiting time has a ranked value of 0.003017600169 and lies within the interval [0.0029708494715480, 0.0029949969211290].

The narrow intervals indicate that the intuitionistic fuzzy representation gives a more compact and stable estimate of the queueing measures. Since intuitionistic fuzzy modelling includes both membership and non-membership information, the uncertainty is represented more precisely. Hence, Node-1 remains lightly loaded and shows stable performance under the triangular intuitionistic fuzzy framework.

Figure 5.2.2 (a) : β-Cut based System Length (LN2) in Robust and Wings span of Triangular Intuitionistic Fuzzy Number

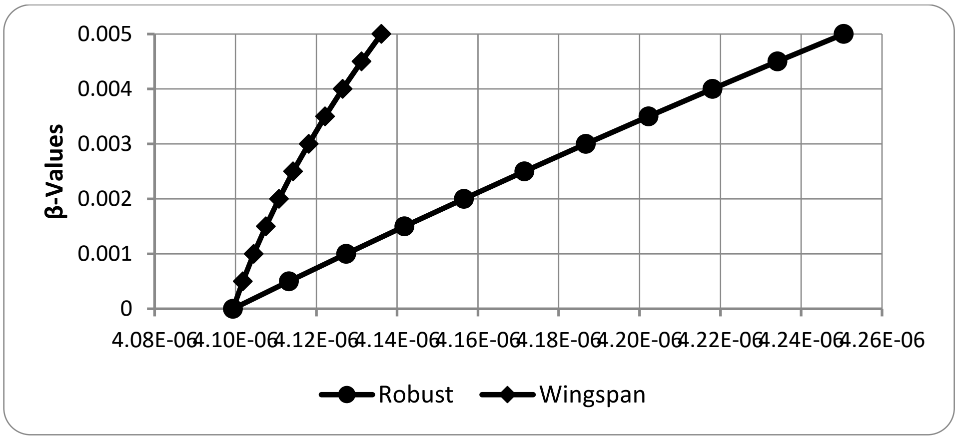

Figure 5.2.2 (b) : β-Cut based Waiting Time (WN2) in Robust and Wings span of Triangular Intuitionistic Fuzzy Number

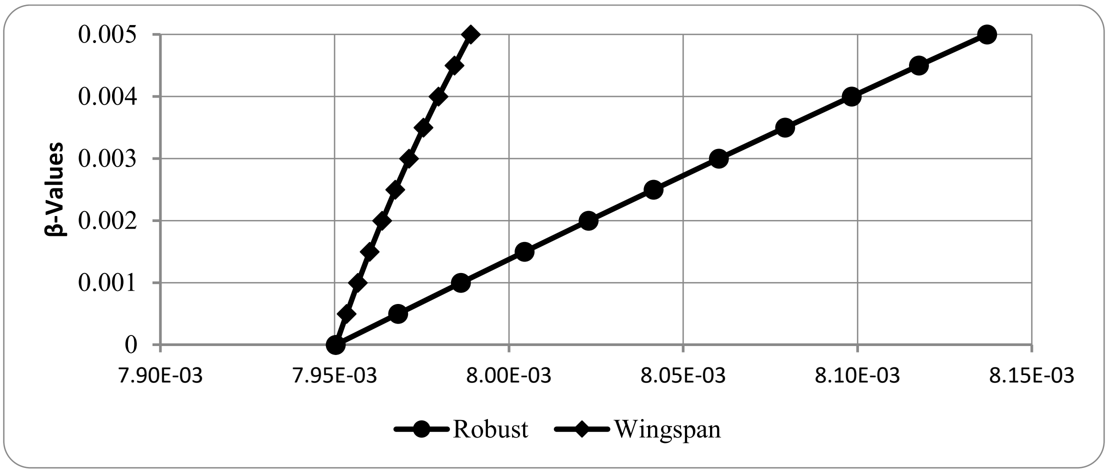

From graph 5.2.2(a) and 5.2.2(b) for Node-2, the expected length has a ranked value of 0.000004164127, lying within the interval [0.0000040993954158, 0.0000041361107602]. The mean waiting time has a ranked value of 0.008075894209, lying within the interval [0.0079503534884140, 0.0081371971421635].

The results show that Node-2 has higher congestion than Node-1, but the uncertainty range is considerably smaller under the intuitionistic fuzzy approach. This demonstrates that the β-cut based ranking procedure provides more controlled estimates of the system performance. The small gap between the robust ranking and wingspan values suggests that the model gives consistent performance estimates for Node-2.

Figure 5.2.3 (a) : β -Cut based System Length (LHO) in Robust and Wings span of Triangular Intuitionistic Fuzzy Number

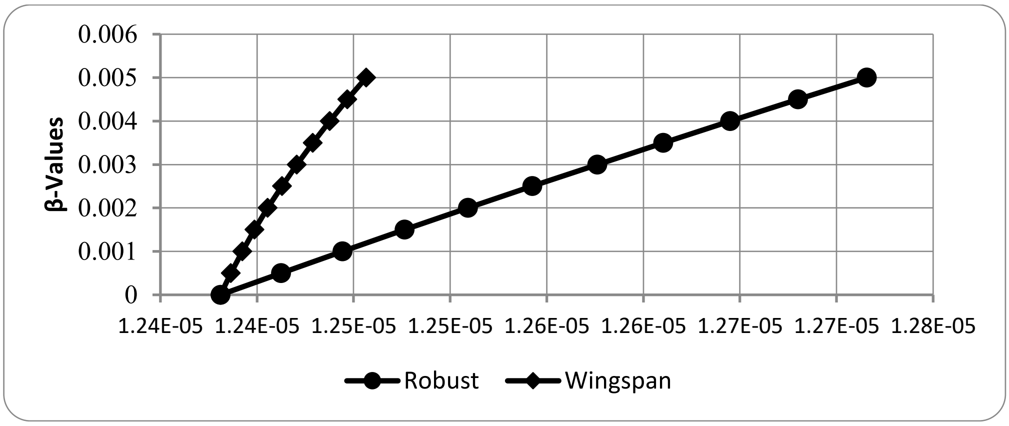

Figure 5.2.3 (b) : β-Cut based Waiting Time (WHO) in Robust and Wings span of Triangular Intuitionistic Fuzzy Number

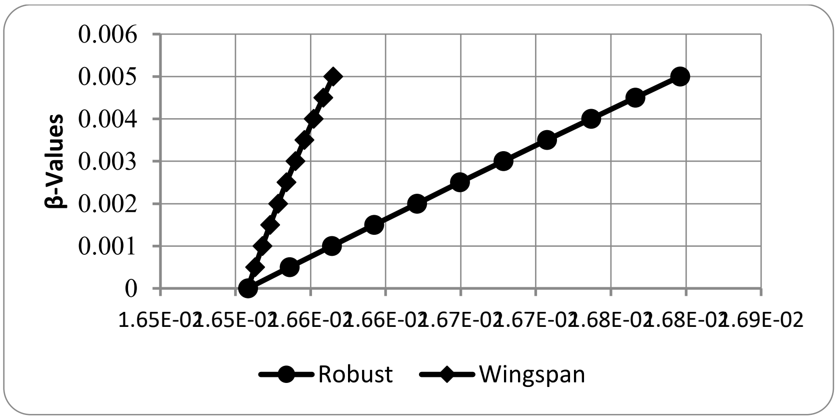

From graph 5.2.3(a) and 5.2.3(b), the Central Server again records the largest system length and waiting time. The expected length has a ranked value of 0.000012581627 and lies within the interval [0.0000123810936768, 0.0000127157216591]. The mean waiting time has a ranked value of 0.016775572796 and lies within the interval [0.0165081930322366, 0.0167959276371549].

Although the Central Server remains the most congested location, the intuitionistic fuzzy results show much narrower intervals than the ordinary triangular fuzzy case. This indicates that the inclusion of hesitation through intuitionistic fuzzy modelling improves the precision of performance evaluation. The Central Server should still be considered the critical bottleneck because it receives cumulative traffic from multiple sources.

Trapezoidal Fuzzy Number

Let us consider an FM/FM/1, Jackson network queueing system with two nodes and one Central Server. Suppose the arrivals rates and service rates are Trapezoidal fuzzy numbers and are represented as

α = [0, 0.1, 0.2, 0.3, 0.4, 0.5, 0.6, 0.7, 0.8, 0.9, 1]

λ_x = [0.008, 0.0099, 0.0101, 0.012]; λ_y = [0.013, 0.0144, 0.0152, 0.017];

λ_h = [0.018, 0.0198, 0.0202, 0.022]

μ_x = [0.018, 0.0198, 0.0202, 0.022]; μ_y = [0.023, 0.0248, 0.0252, 0.027];

μ_h = [0.028, 0.0298, 0.0302, 0.032]

For a given range of values of α, λx, λy, λy, μx, μy and μh the expected length of the system at each node and Central Server and waiting times at respective areas are shown from Graphs 5.3.1(a), 5.3.1(b) to 5.3.3(a), 5.3.3(b) by keeping values of other parameters fixed.

Figure 5.3.1 (a) : α-Cut based System Length (LN1) in Robust and Wings span of Trapezoidal fuzzy

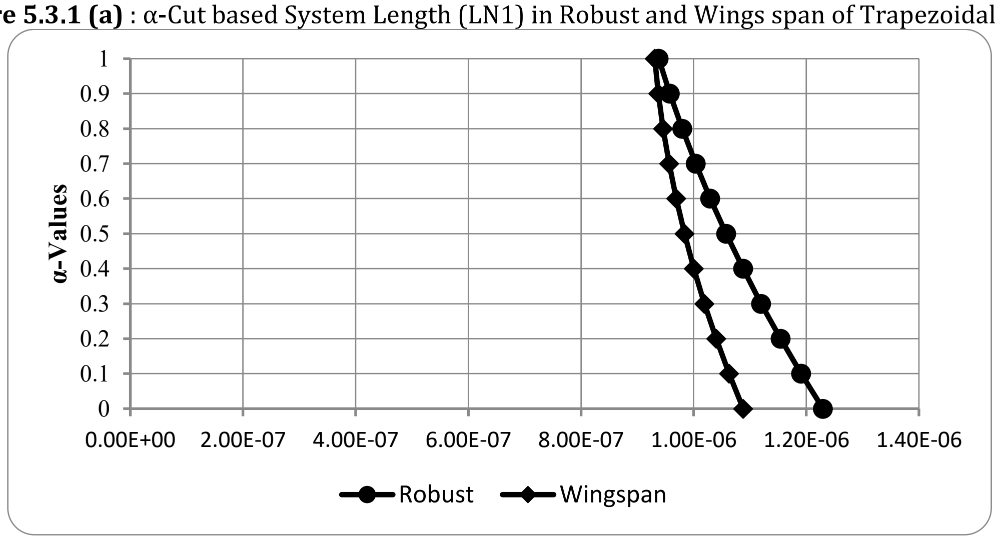

Figure 5.3.1 (b) : α-Cut based Waiting Time (WN1) in Robust and Wings span of Trapezoidal fuzzy

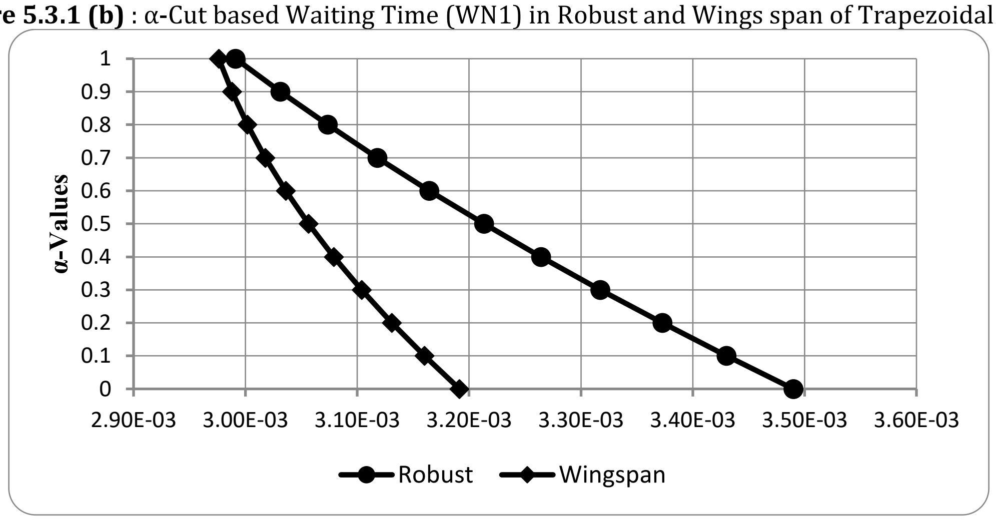

From graph 5.3.1(a) and 5.3.1(b), for the trapezoidal fuzzy case, the expected length at Node-1 has a ranked value of 0.000000943000 and lies within the interval [0.0000009380474191, 0.0000010880493004]. The mean waiting time has a ranked value of 0.003017600169 and lies within the interval [0.0029912463497116, 0.0031914080850799].

The results show that Node-1 has low congestion and stable waiting-time behaviour under trapezoidal fuzzy parameters. Compared with triangular fuzzy numbers, the trapezoidal fuzzy representation provides a more controlled uncertainty range because of the presence of a wider core region. This makes trapezoidal fuzzy modelling useful when the arrival and service rates are not represented by a single most likely value but by a range of most plausible values.

Figure 5.3.2 (a) : α-Cut based System Length (LN2) in Robust and Wings span of Trapezoidal fuzzy

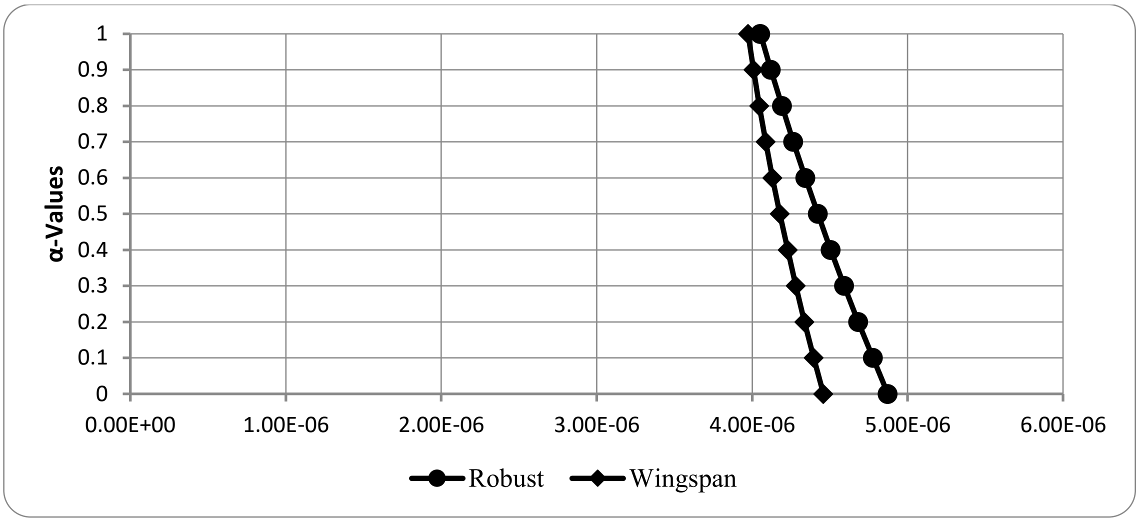

Figure 5.3.2 (b) : α-Cut based Waiting Time (WN2) in Robust and Wings span of Trapezoidal fuzzy

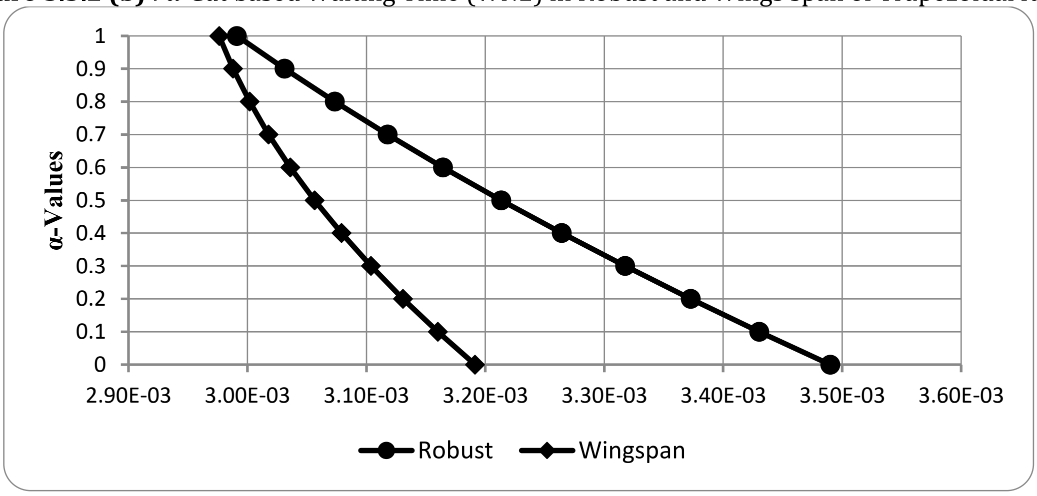

From graph 5.3.2(a) and 5.3.2(b), at Node-2, the expected length has a ranked value of 0.000004164127 and lies within the interval [0.0000039736223689, 0.0000048730369418]. The mean waiting time has a ranked value of 0.008075894209 and lies within the interval [0.0077818201814066, 0.0088064765788292].

The results indicate that Node-2 has greater congestion than Node-1. However, the trapezoidal fuzzy representation keeps the uncertainty range within a moderate interval. The increasing α-cut level reduces uncertainty and gives more reliable ranked estimates. This confirms that ranking-based analysis can identify differences in node-wise congestion even when system parameters are imprecise.

Figure 5.3.3 (a) : α-Cut based System Length (LHO) in Robust and Wings span of Trapezoidal fuzzy

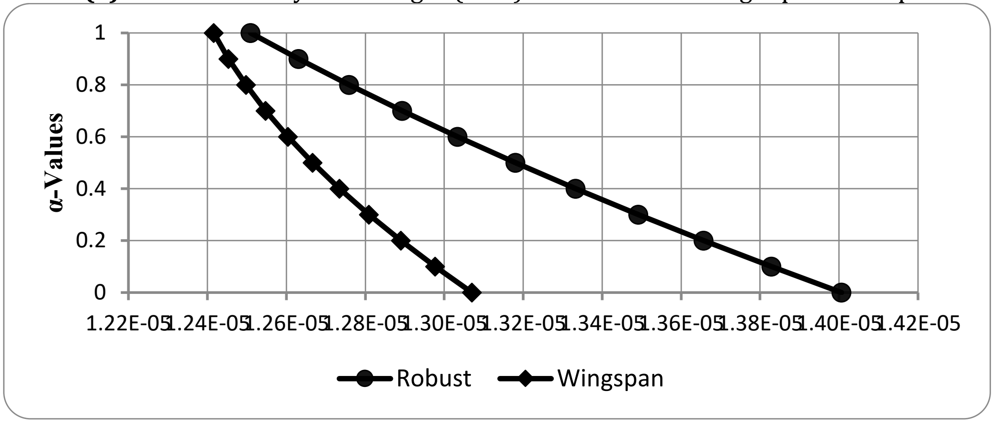

Figure 5.3.3 (b) : α-Cut based Waiting Time (WHO) in Robust and Wings span of Trapezoidal fuzzy

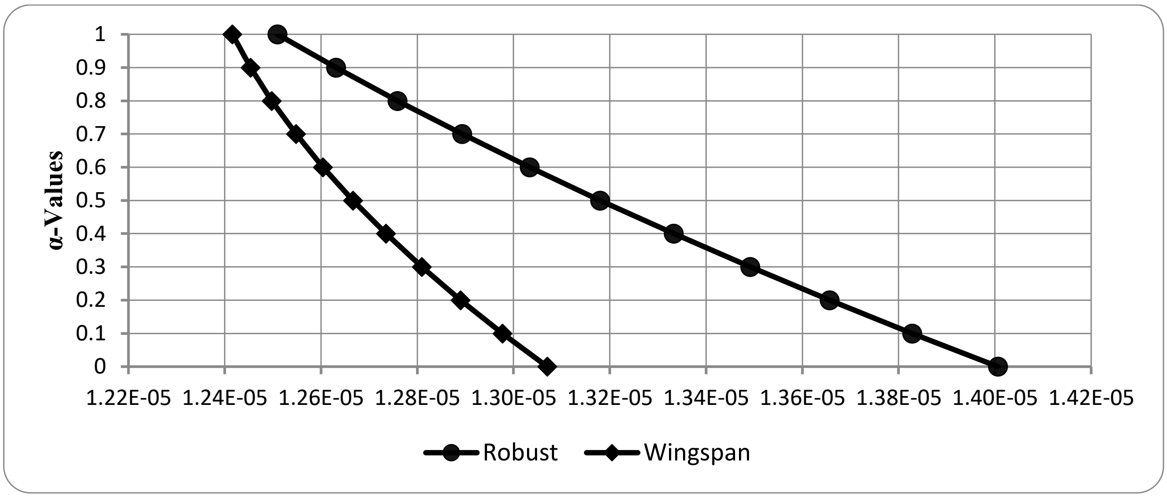

From graph 5.3.2(a) and 5.3.2(b), the Central Server has a ranked expected length of 0.000012581627, lying within the interval [0.0000124160392129, 0.0000140063317211]. The ranked mean waiting time is 0.016775572796, lying within the interval [0.0165377045263243, 0.0177867041052240].

These results confirm that the Central Server is the most heavily loaded component of the network. The larger values of expected length and waiting time are due to the combined effect of external arrivals and routed traffic from Node-1 and Node-2. Although trapezoidal fuzzy modelling reduces the spread compared with the triangular fuzzy case, the Central Server still remains the main congestion point. Therefore, system improvement should focus primarily on increasing service efficiency at the Central Server.

Trapezoidal Intuitionistic Fuzzy Number

Let us consider an IFM/IFM/1, Jackson network queueing system with two nodes and one Central Server. Suppose the arrivals rates and service rates are Trapezoidal fuzzy numbers and are represented as

Beta(β) = [0, 0.0005, 0.001, 0.0015, 0.002, 0.0025, 0.003, 0.0035, 0.004, 0.0045, 0.005]
λ_x = [0.008, 0.0099, 0.0101, 0.012]; λ_y = [0.013, 0.0144, 0.0152, 0.017];
λ_h = [0.018, 0.0198, 0.0202, 0.022]
μ_x = [0.018, 0.0198, 0.0202, 0.022]; μ_y = [0.023, 0.0248, 0.0252, 0.027];
μ_h = [0.028, 0.0298, 0.0302, 0.032]

For a given range of values of α, λx, λy, λy, μx, μy and μh the expected length of the system at each node and Central Server and waiting times at respective areas are shown from Graphs 5.4.1(a), 5.4.1(b) to 5.4.3(a), 5.4.3(b) by keeping values of other parameters fixed.

Figure 5.4.1 (a) : β-Cut based System Length (LN1) in Robust and Wings span of Trapezoidal Intuitionistic fuzzy Number

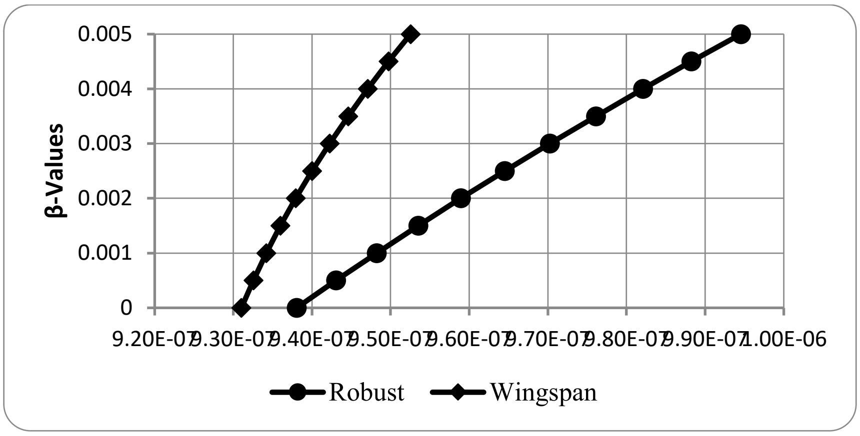

Figure 5.4.1 (b) : β-Cut based System Length (WN1) in Robust and Wings span of Trapezoidal Intuitionistic fuzzy Number

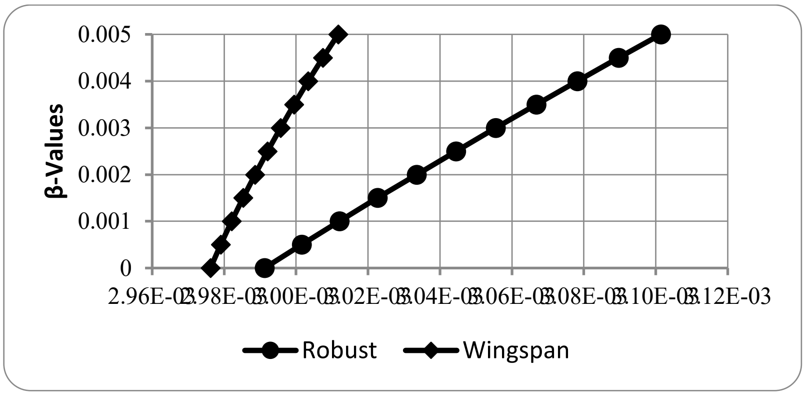

From graph 5.4.1(a) and 5.4.1(b), for Node-1 under the trapezoidal intuitionistic fuzzy environment, the expected system length has a ranked value of 0.000000943000 and lies within the interval [0.00000093101957, 0.0000009945451267]. The mean waiting time has a ranked value of 0.003017600169 and lies within the interval [0.00297618514197, 0.0031013859349392].

The results indicate that Node-1 maintains stable performance with very low congestion. The interval width is small, showing that trapezoidal intuitionistic fuzzy modelling provides a refined representation of uncertainty. The combined use of trapezoidal fuzzy numbers and intuitionistic fuzzy information improves the reliability of the ranked performance measures.

Figure 5.4.2 (a) : β-Cut based System Length (LN2) in Robust and Wings span of Trapezoidal Intuitionistic fuzzy Number

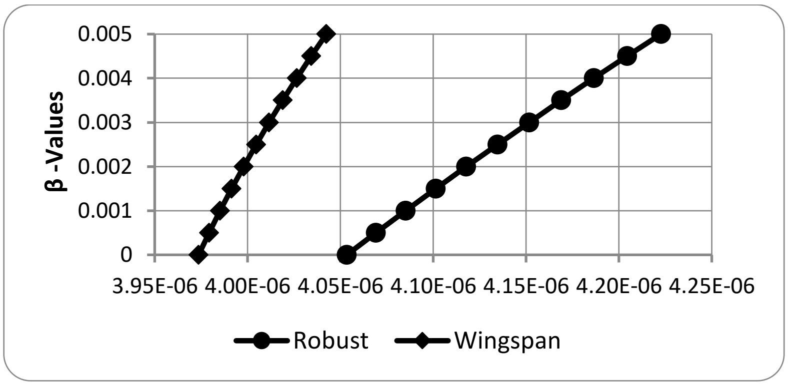

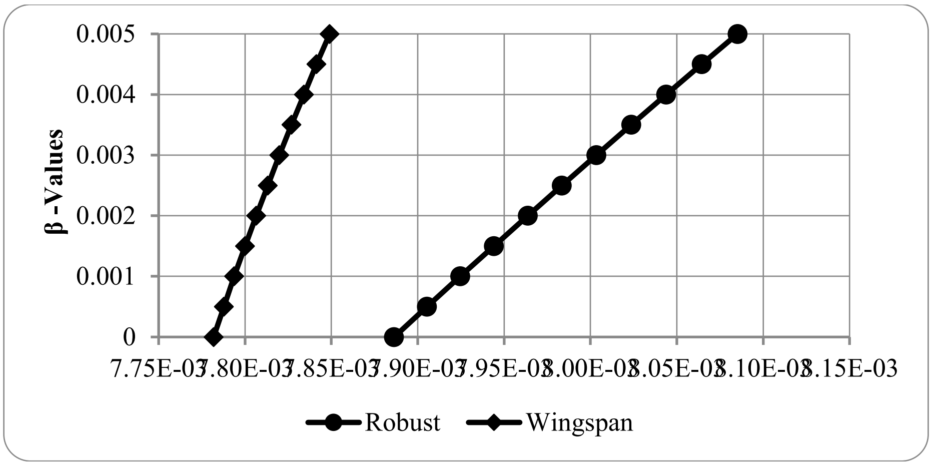

Figure 5.4.2 (b) : β-Cut based Waiting Time (WN2) in Robust and Wings span of Trapezoidal Intuitionistic fuzzy Number

From graph 5.4.2(a) and 5.4.2(b),For Node-2, the expected system length has a ranked value of 0.000004164127 and lies within the interval [0.00000397362237, 0.0000042226671109]. The mean waiting time has a ranked value of 0.008075894209 and lies within the interval [0.00778182018141, 0.0080851526336308].

Results indicate that for Node-2 there is moderate congestion, which is in comparison to Node-1. But the interval of uncertainty is small, and that means that the trapezoidal intuitionistic fuzzy ranking method provides more precise estimates on the values of performance measures. This helps to justify the practicability of the method for analysing queueing system in which both uncertainty and hesitation exist when estimating the parameters..

Figure 5.4.3 (a) : β-Cut based System Length (LHO) in Robust and Wings span of Trapezoidal Intuitionistic fuzzy Number

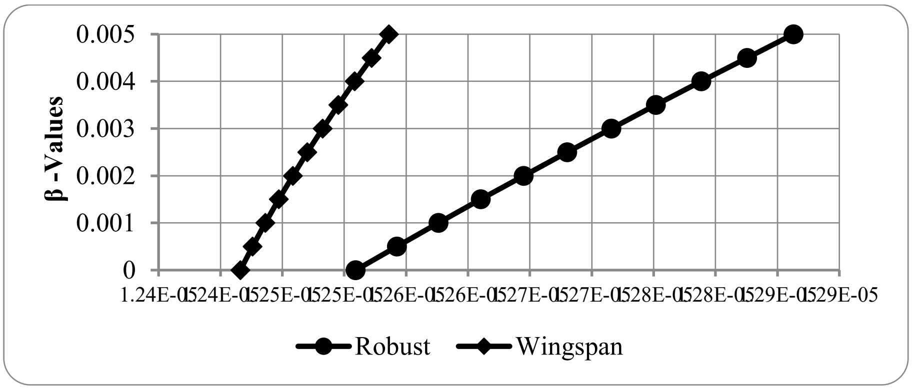

Figure 5.4.3 (b) : β-Cut based Waiting Time (WHO) in Robust and Wings span of Trapezoidal Intuitionistic fuzzy Number

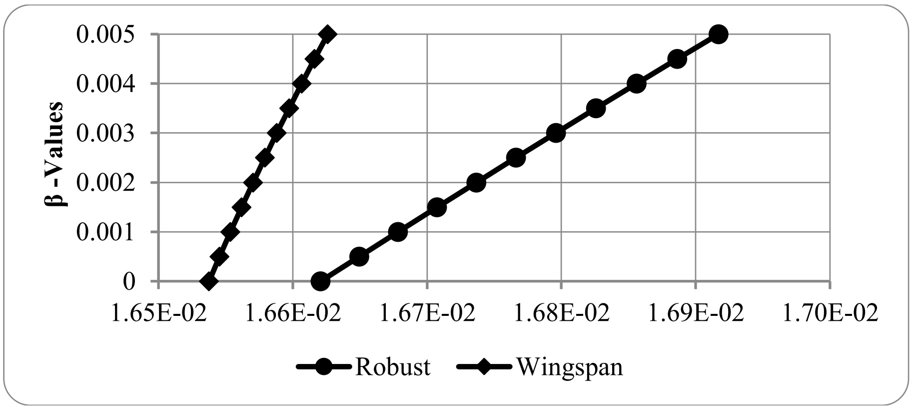

From graph 5.4.2(a) and 5.4.2(b), the Central Server has a ranked expected system length of 0.000012581627, lying within the interval [0.00001241603921, 0.0000128629160589]. The mean waiting time has a ranked value of 0.016775572796 and lies within the interval [0.01653770452632, 0.0169170558796621].

The Central Server continues to show the highest level of congestion in the network. However, the trapezoidal intuitionistic fuzzy results produce comparatively narrow intervals, indicating better control over uncertainty. This is a confirmation that Central Server is the major bottleneck, but the proposed ranking based approach is a more reliable performance estimation of the Central Server under uncertain operating environment.

Discussion

Effect of Triangular Fuzzy Parameters

The triangular fuzzy results show that the expected system length and mean waiting time decrease as the α-cut value increases. This indicates that the uncertainty in arrival and service rates reduces at higher α levels. Under triangular fuzzy parameters, the performance measures are more spread at lower α values, showing higher uncertainty in the queueing behaviour. The results also indicate that the Central Server has higher congestion than Node-1 and Node-2 due to the combined effect of direct arrivals and routed task from both nodes.

Effect of Triangular Intuitionistic Fuzzy Parameters

In the triangular intuitionistic fuzzy case, the β-cut based results show a narrow range of variation in system length and waiting time. This indicates that the intuitionistic fuzzy approach provides a more refined representation of uncertainty by considering membership, non-membership and hesitation degree. Compared with the ordinary triangular fuzzy case, the triangular intuitionistic fuzzy results are more compact and stable. This shows that intuitionistic fuzzy modelling improves the reliability of ranking-based queueing performance analysis.

Effect of Trapezoidal Fuzzy Parameters

The trapezoidal fuzzy results exhibit more stable pattern than the triangular fuzzy. The trapezoidal fuzzy numbers have a core range, which mean the range of most possible values is comparatively small and also the uncertainty interval is small. The closer the robust ranking and wingspan values the higher the α-cut value leading to better accuracy in the performance measures. The results indicate the usefulness of trapezoidal fuzzy modelling when the parameters of the system are not a single value but a range of possible values.

Effect of Trapezoidal Intuitionistic Fuzzy parameters

The case of trapezoidal intuitionistic fuzzy results gives the most stable and controlled estimates in comparison to the cases considered. The range of system times and mean waiting times are smaller, indicating a better control of the uncertainty. The use of trapezoidal fuzzy numbers in the intuitionistic fuzzy modelling yields greater precision as it represents a range of likely values, in addition to the degree of hesitation. Therefore this method can be applied to the study of queueing systems with a large level of parameter uncertainty.

Effect of α-cut and β-cut Values

It can be seen that in the α-cut results, when the α value is increased from 0 to 1, the uncertainty interval of the queueing measures becomes smaller. Low values of alpha indicate a large spectrum of possible system behaviour and high values of alpha indicate more confident and accurate estimates. Thus it can be seen that higher values of α result in lower values of fuzziness of the expected system length and the mean waiting time. This validates the use of α-cut analysis to gain insight into the influence of uncertainty on the queueing network performance.

The β-cut in the intuitionistic fuzzy environment exhibits the influence of the hesitation and non-membership on the system performance. The values for robust ranking and wingspan are in a fairly small range as β changes, suggesting that the performance estimates have not varied much. The β-cut based analysis is able to provide more information than the usual fuzzy based analysis since it models uncertainty on both acceptance and rejection sides. Therefore, the usage of β-cut analysis helps to interpret the behaviour of queuing performance in intuitionistic fuzzy situation.

Node-wise performance comparison

The lowest expected system length of the three service points is at node-1 and the mean waiting time is also the lowest of the three. This means it is the least busy point of the network: Node-1. As can be seen in the graphical results, the higher α or β is, the lower the uncertainty. The values of the ranked scores are still relatively small. Thus, it can be stated that Node-1 is a stable service node with relatively better performance for both fuzzy and intuitionistic fuzzy environment.

Node-2 shows higher expected system length and waiting time than Node-1. This suggests that Node-2 experiences moderate congestion under the assumed arrival and service conditions. The results indicate that uncertainty in Node-2 performance is also reduced at higher α-cut and β-cut levels. Although Node-2 is not the most congested part of the system, it requires more attention than Node-1 because its waiting time and system length are comparatively higher.

The Central Server shows the highest expected system length and mean waiting time in all fuzzy and intuitionistic fuzzy cases. This is because the Central Server receives both external arrivals and routed task from Node-1 and Node-2. The graphical results clearly indicate that the Central Server is the major congestion point of the network. Therefore, improvement in service capacity at the Central Server may reduce the overall waiting time and improve the performance of the entire queueing system.

Conclusion

This study presented a ranking-based performance analysis of an M/M/1 Jackson network queueing system with task impatience under fuzzy and intuitionistic fuzzy environments. The expected system length and mean waiting time were evaluated for Node-1, Node-2 and the Central Server by using robust ranking and wingspan methods. The results showed that the uncertainty in the performance measures decreases as the α-cut value increases in fuzzy models, while β-cut based intuitionistic fuzzy results provide more stable and compact intervals by incorporating membership, non-membership and hesitation information.

Trapezoidal fuzzy and trapezoidal intuitionistic fuzzy models resulted in more controlled uncertainty ranges compared with the triangular fuzzy models among the cases considered. The intuitionistic fuzzy approach provided more reliable and precise estimates as it encompassed more uncertainty information. In all the graphical results, the congestion of Node-1 was the lowest, the congestion of Node-2 was moderate, and the congestion of the Central Server was the highest with the greatest expected system length and waiting time. This means that, there are direct task arrivals and routed task from both the nodes, which implies that the major bottleneck of the network is the Central Server.

The findings are relevant for the study of computer networks, cloud services, and distributed processing systems, among other applications, in the context of congestion, processing delay, task abandonment and resource consumption. The proposed ranking-based approach is a practical tool for comparing uncertain queueing performance measures that enable the identification of the overloaded processing units. It can be used to assist the network designer and system administrator in determining the capacity of services, optimize their routing decisions, and enhance their task scheduling policies and minimise waiting time under uncertain traffic and service conditions. Overall, the study demonstrates that robust ranking and wingspan methods are effective for performance evaluation and congestion-aware capacity planning in modern computer networks, cloud systems and distributed computing environments.

Limitation of Study: This study is limited to a finite-capacity Jackson-type network with two processing nodes and one central server. The arrival and service processes are assumed to follow Markovian assumptions. The routing structure is restricted from individual nodes to the central server, and feedback routing between nodes is not considered. Future studies may extend the model to multi-server networks, priority scheduling, cloud-edge architectures, real-time traffic datasets and simulation-based validation

Conflict of Interest: None to declare

Funding: None

Authors Contribution: Sachin R. Gurnule contributed to, model development, numerical implementation, analysis, and drafting. V.N. Rama Devi contributed to conceptualization, supervision, validation, methodological review, interpretation, and manuscript revision. P. Pranay contributed to study design, model refinement, mathematical guidance, verification, and editing.

Acknowledgement: The first author is thankful to the Head and Faculty members of Department of Mathematics and Statistics, Chaitanya (DU), Guide and Co-guide for their encouragement and Constant support.

References

1. Erlang AK. Solution of some problems in the theory of probabilities of significance in automatic telephone exchanges. Post Office Electrical Engineers' Journal. 1917-1918; 10:189-197.

2. Burke PJ. The output of a queueing system. Oper Res. 1956;4(6):699-704. doi:10.1287/opre.4.6.699.
3. Jackson JR. Networks of waiting lines. Oper Res. 1957;5(4):518-521. doi:10.1287/opre.5.4.518.
4. Jackson JR. Jobshop-like queueing systems. Manage Sci. 1963;10(1):131-142. doi:10.1287/mnsc.10.1.131.
5. Gordon WJ, Newell GF. Closed queueing systems with exponential servers. Oper Res. 1967;15(2):254-265. doi:10.1287/opre.15.2.254.
6. Baskett F, Chandy KM, Muntz RR, Palacios FG. Open, closed, and mixed networks of queues with different classes of customers. J ACM. 1975;22(2):248-260. doi:10.1145/321879.321887.
7. Kleinrock L. Queueing Systems. Vol 1, Theory. New York: John Wiley & Sons; 1975.
8. Kleinrock L. Queueing Systems. Vol 2, Computer Applications. New York: John Wiley & Sons; 1976.
9. Lazowska ED, Zahorjan J, Graham GS, Sevcik KC. Quantitative System Performance Computer System Analysis Using Queueing Network Models [Internet]. [cited 2026 Jun 24]. Available from: https://ifotechpoly.edu.ng/elibrary/elibrary/computer_hardware_engineering/Quantitative%20System%20Performance.pdf
10. Whitt W. Open and closed models for networks of queues. AT&T Bell Lab Tech J. 1984;63(9):1911-1979. doi:10.1002/j.1538-7305.1984.tb00084.x.
11. Down D, Bolch G, Greiner S, Meer HD, Trivedi K. Queueing Networks and Markov Chains: Modeling and Performance Evaluation with Computer Science Applications. Journal of the American Statistical Association. 2000 Mar;95(449):346.
12. Harchol-Balter M. Performance Modeling and Design of Computer Systems: Queueing Theory in Action. Cambridge: Cambridge University Press; 2013.
13. Atiquzzaman M. Special Issue: Enterprise Networks. Computer Communications. 1999 Sep;22(14):1281–2.
14. Zadeh LA. Fuzzy sets. Inf Control. 1965;8(3):338-353. doi:10.1016/S0019-9958(65)90241-X.
15. Bellman RE, Zadeh LA. Decision-Making in a Fuzzy Environment. Management Science. 1970 Dec;17(4):B-141-B-164.
16. Zimmermann HJ. Fuzzy Set Theory and Its Applications. 4th ed. Boston: Springer; 2001. Available from: https://archive.org/details/HJZimmermannauthFuzzySetTheory--andItsApplications2001/page/n3/mode/2up
17. Atanassov KT. Intuitionistic fuzzy sets. Fuzzy Sets Syst. 1986;20(1):87-96. doi:10.1016/S0165-0114(86)80034-3.
18. Li RJ, Lee ES. Analysis of fuzzy queues. Comput Math Appl. 1989;17(7):1143-1147. doi:10.1016/0898-1221(89)90044-8.
19. Negi DS, Lee ES. Analysis and simulation of fuzzy queues. Fuzzy Sets Syst. 1992;46(3):321-330. doi:10.1016/0165-0114(92)90370-J.
20. Kao C, Li CC, Chen SP. Parametric programming to the analysis of fuzzy queues. Fuzzy Sets Syst. 1999;107(1):93-100. doi:10.1016/S0165-0114(97)00295-9.
21. Chen SP. Parametric nonlinear programming approach to fuzzy queues with bulk service. Eur J Oper Res. 2005;163(2):434-444. doi:10.1016/j.ejor.2003.10.038.
22. Chen SH. Ranking fuzzy numbers with maximizing set and minimizing set. Fuzzy Sets Syst. 1985;17(2):113-129. doi:10.1016/0165-0114(85)90050-8.
23. Yager RR. A procedure for ordering fuzzy subsets of the unit interval. Inf Sci. 1981;24(2):143-161. doi:10.1016/0020-0255(81)90017-7.
24. Liou TS, Wang MJ. Ranking fuzzy numbers with integral value. Fuzzy Sets Syst. 1992;50(3):247-255. doi:10.1016/0165-0114(92)90223-Q.
25. Xu Z. Some similarity measures of intuitionistic fuzzy sets and their applications to multiple attribute decision making. Fuzzy Optim Decis Mak. 2007;6(2):109-121. doi:10.1007/s10700-007-9004-z. 21), p.5573. https://doi.org/10.3390/en18215573

Appendix 1 : Derived Kolmogorov forward differential equations

The Transient state equations governing the various probabilities are detailed in the form of following Differential equations:

1. $\frac{dp^{(t)}_{(0.0.0)}}{dt} = -(\lambda_x b_1 + \lambda_y b_2 + \lambda_h b_3)\ p^{(t)}_{(0.0.0)} + \mu_x(1-\mathrm{p}_1)\,p^{(t)}_{(1.0.0)} + \mu_y(1-\mathrm{p}_2)\,p^{(t)}_{(0.1.0)} + \mu_h\, p^{(t)}_{(0.0.1)}$
2. $\frac{dp^{(t)}_{(j.0.0)}}{dt} = -(\lambda_x b_1 + (\mu_x + (\mathrm{j}-1)\xi_1) + \lambda_y b_2 + \lambda_h b_3)\mathrm{P}^{(t)}_{(\mathrm{j},0,0)} + \lambda_x b_1 \mathrm{P}^{(t)}_{(\mathrm{j}-1,0,0)} + \mu_x(1-\mathrm{p}_1)\mathrm{P}^{(t)}_{(\mathrm{j}+1,0,0)} + \mu_y(1-\mathrm{p}_2)\mathrm{P}^{(t)}_{(\mathrm{j},1,0)} + \mu_h \mathrm{P}^{(t)}_{(\mathrm{j},0,1)}\ ;\ 1 \le j \le s-1$
3. $\frac{dP^{(t)}_{(s,0,0)}}{dt} = -(\lambda_y b_2 + (\mu_x + (\mathrm{s}-1)\xi_1) + \lambda_h b_3)\mathrm{P}^{(t)}_{(\mathrm{s},0,0)} + \lambda_x b_1 \mathrm{P}^{(t)}_{(\mathrm{s}-1,0,0)} + \mu_y(1-\mathrm{p}_2)\mathrm{P}^{(t)}_{(\mathrm{s},1,0)} + \mu_h \mathrm{P}^{(t)}_{(\mathrm{s},0,1)}$

4. $\frac{dP^{(t)}_{(0,k,0)}}{dt} = -(\lambda_x b_1 + (\mu_y + (k-1)\xi_2) + \lambda_y b_2 + \lambda_h b_3)P^{(t)}_{(0,k,0)} + \lambda_y b_2 P^{(t)}_{(0,k-1,0)} + (\mu_y(1-p_2) + k\xi_2)P^{(t)}_{(0,k+1,0)} + \mu_x(1-p_1)P^{(t)}_{(1,k,0)} + \mu_h P^{(t)}_{(0,k,1)};\ 1 \le k \le s-1$
5. $\frac{dP^{(t)}_{(0,s,0)}}{dt} = -(\lambda_x b_1 + (\mu_y + (s-1)\xi_2) + \lambda_h b_3)P^{(t)}_{(0,s,0)} + \lambda_y b_2 P^{(t)}_{(0,s,0)} + \mu_x(1-p_1)P^{(t)}_{(1,s,0)} + \mu_h P^{(t)}_{(0,s,1)}$
6. $\frac{dP^{(t)}_{(0,0,h)}}{dt} = -(\lambda_x b_1 + (\mu_h + (h-1)\xi_3 + \lambda_y b_2 + \lambda_h b_3)P^{(t)}_{(0,0,h)} + \lambda_h b_3 P^{(t)}_{(0,s,h-1)} + (\mu_h + h\xi_3))P^{(t)}_{(0,0,h+1)} + \mu_x p_1 P^{(t)}_{(1,0,h-1)} + \mu_y p_2 P^{(t)}_{(0,1,h-1)};\ 1 \le h \le s-1$
7. $\frac{dP^{(t)}_{(0,0,s)}}{dt} = -(\lambda_x b_1 + \lambda_y b_2 + (\mu_h + (s-1)\xi_3)P^{(t)}_{(0,0,s)} + \lambda_h b_3 P^{(t)}_{(0,0,s-1)} + \mu_x p_1 P^{(t)}_{(1,0,s-1)} + \mu_y p_2 P^{(t)}_{(0,1,s-1)}$
8. $\frac{dP^{(t)}_{(j,k,0)}}{dt} = -(\lambda_x b_1 + (\mu_x + (j-1)\xi_1) + \lambda_y b_2 + (\mu_y + (k-1)\xi_2) + \lambda_h b_3)P^{(t)}_{(j,k,0)} + (\mu_x(1-p_1) + j\xi_1)P^{(t)}_{(j+1,k,0)} + (\mu_y(1-p_2) + k\xi_2)P^{(t)}_{(j,k+1,0)} + \lambda_x b_1 P^{(t)}_{(j-1,k,0)} + \lambda_y b_2 P^{(t)}_{(j,k-1,0)} + +\mu_h P^{(t)}_{(j,k,1)};\ 1 \le j \le s-1, 1 \le k \le s-1$
9. $\frac{dP^{(t)}_{(j,s,0)}}{dt} = -(\lambda_x b_1 + (\mu_x + (j-1)\xi_1) + (\mu_y + (s-1)\xi_2) + \lambda_h b_3)P^{(t)}_{(j,s,0)} + (\mu_x(1-p_1) + j\xi_1)P^{(t)}_{(j+1,s,0)} + \lambda_x b_1 P^{(t)}_{(j-1,s,0)} + \lambda_y b_2 P^{(t)}_{(j,s-1,0)} + \mu_h P^{(t)}_{(j,s,1)};\ 1 \le j \le s-1$
10. $\frac{dP^{(t)}_{(s,k,0)}}{dt} = -((\mu_x + (s-1)\xi_1) + \lambda_y b_2 + (\mu_y + (k-1)\xi_2) + \lambda_h b_3)P^{(t)}_{(s,k,0)} + (\mu_y(1-p_2) + k\xi_2)P^{(t)}_{(s,k+1,0)} + \lambda_y b_2 P^{(t)}_{(s,k-1,0)} + \lambda_x b_1 P^{(t)}_{(s-1,k,0)} + \mu_h P^{(t)}_{(s,k,1)};\ 1 \le k \le s-1$
11. $\frac{dP^{(t)}_{(s,s,0)}}{dt} = -((\mu_x + (s-1)\xi_1) + (\mu_y + (s-1)\xi_2) + \lambda_h b_3)P^{(t)}_{(s,s,0)} + \lambda_x b_1 P^{(t)}_{(s-1,s,0)} + \lambda_y b_2 P^{(t)}_{(s,s-1,0)}$
12. $\frac{dP^{(t)}_{(0,k,h)}}{dt} = -(\lambda_x b_1 + \lambda_y b_2 + (\mu_y + (k-1)\xi_2) + \lambda_h b_3 + (\mu_h + (h-1)\xi_3))P^{(t)}_{(0,k,h)} + \mu_x(1-p_1)P^{(t)}_{(1,k,h)} + \mu_y(1-p_2)P^{(t)}_{(0,k+1,h)} + (\mu_h + h\xi_3)P^{(t)}_{(0,k,h+1)} + \lambda_h b_3 P^{(t)}_{(0,k,h-1)} + \lambda_y b_2 P^{(t)}_{(0,k-1,h)};\ 1 \le k \le s-1, 1 \le h \le s-1$
13. $\frac{dP^{(t)}_{(0,s,h)}}{dt} = -(\lambda_x b_1 + (\mu_y + (s-1)\xi_2) + \lambda_h b_3 + (\mu_h + (h-1)\xi_3))P^{(t)}_{(0,s,h)} + (\mu_h + h\xi_3)P^{(t)}_{(0,s,h+1)} + \lambda_h b_3 P^{(t)}_{(0,s,h-1)} + \lambda_y b_2 P^{(t)}_{(0,s,h)} + \mu_x(1-p_1)P^{(t)}_{(1,s,h)};\ 1 \le h \le s-1$
14. $\frac{dP^{(t)}_{(0,k,s)}}{dt} = -(\lambda_x b_1 + \lambda_y b_2 + (\mu_y + (k-1)\xi_2) + (\mu_h + (s-1)\xi_3))P^{(t)}_{(0,k,s)} + (\mu_y(1-p_2) + k\xi_2)P^{(t)}_{(0,k+1,s)} + \lambda_h b_3 P^{(t)}_{(0,k,s-1)} + \lambda_y b_2 P^{(t)}_{(0,k-1,s)} + \mu_x(1-p_1)P^{(t)}_{(1,s,h)};\ 1 \le k \le s-1$
15. $\frac{dP^{(t)}_{(0,s,s)}}{dt} = -(\lambda_x b_1 + (\mu_y + (s-1)\xi_2) + (\mu_h + (s-1)\xi_3))P^{(t)}_{(0,s,s)} + \lambda_h b_3 P^{(t)}_{(0,s,s-1)} + \lambda_y b_2 P^{(t)}_{(0,s-1,s)} + \mu_x(1-p_1)P^{(t)}_{(1,s,s)};\ 1 \le k \le s-1$
16. $\frac{dP^{(t)}_{(j,0,h)}}{dt} = -(\lambda_x b_1 + (\mu_x + (j-1)\xi_1) + \lambda_y b_2 + \lambda_h b_3 + (\mu_h + (h-1)\xi_3))P^{(t)}_{(j,0,h)} + (\mu_x(1-p_1) + j\xi_1)P^{(t)}_{(j+1,0,h)} + (\mu_h + h\xi_3)P^{(t)}_{(j,0,h+1)} + \lambda_x b_1 P^{(t)}_{(j-1,0,h)} P(j-1,0,h) + \lambda_h b_3 P^{(t)}_{(j,0,h-1)} + \mu_y(1-p_2)P^{(t)}_{(j,1,h)};\ 1 \le j \le s-1, 1 \le h \le s-1$
17. $\frac{dP^{(t)}_{(s,0,h)}}{dt} = -((\mu_x + (s-1)\xi_1) + \lambda_y b_2 + \lambda_h b_3 + (\mu_h + (h-1)\xi_3))P^{(t)}_{(s,0,h)} + \lambda_x b_1 P^{(t)}_{(s-1,0,h)} + (\mu_h + h\xi_3)P^{(t)}_{(s,0,h+1)} + \lambda_h b_3 P^{(t)}_{(s,0,h-1)} + \mu_y(1-p_2)P^{(t)}_{(s,1,h)};\ 1 \le h \le s-1$
18. $\frac{dP^{(t)}_{(j,0,s)}}{dt} = -(\lambda_x b_1 + (\mu_x + (j-1)\xi_1) + \lambda_y b_2 + (\mu_h + (s-1)\xi_3))P^{(t)}_{(j,0,s)} + \lambda_h b_3 P^{(t)}_{(j,0,s-1)} + (\mu_x(1-p_1) + j\xi_1)P^{(t)}_{(j+1,0,s)} + \lambda_x b_1 P^{(t)}_{(j-1,0,s)} + \mu_y(1-p_2)P^{(t)}_{(j,1,s)};\ 1 \le j \le s-1$
19. $\frac{dP^{(t)}_{(s,0,s)}}{dt} = -((\mu_x + (s-1)\xi_1) + \lambda_y b_2 + (\mu_h + (s-1)\xi_3))P^{(t)}_{(s,0,s)} + \lambda_x b_1 P^{(t)}_{(s,0,s)} + \lambda_h b_3 P^{(t)}_{(s,0,s-1)} + \mu_y(1-p_2)P^{(t)}_{(s,1,s)}$
20. $\frac{dP^{(t)}_{(j,k,h)}}{dt} = -(\lambda_x b_1 + (\mu_x + (j-1)\xi_1) + \lambda_y b_2 + (\mu_y + (k-1)\xi_2) + \lambda_h b_3 + (\mu_h + (h-1)\xi_3))P^{(t)}_{(j,k,h)} + (\mu_x(1-p_1) + (j)\xi_1)P^{(t)}_{(j+1,k,h)} + (\mu_y(1-p_2) + k\xi_2)P^{(t)}_{(j,k+1,h)} + (\mu_h + (h)\xi_3)P^{(t)}_{(j,k,h+1)} + \lambda_x b_1 P^{(t)}_{(j-1,k,h)} + \lambda_y b_2 P^{(t)}_{(j,k-1,h)} + \lambda_h b_3 P^{(t)}_{(j,k,h-1)};\ 1 \le j \le s-1, 1 \le k \le s-1, 1 \le h \le s-1$

21. $\frac{dP^{(t)}_{(s,k,h)}}{dt} = -\big((\mu_x + (s-1)\xi_1) + \lambda_y b_2 + (\mu_y + (k-1)\xi_2) + \lambda_h b_3 + (\mu_h + (h-1)\xi_3)\big)\mathrm{P}^{(t)}_{(s,k,h)} + (\mu_y(1-p_2) + k\xi_2)\mathrm{P}^{(t)}_{(s+1,k+1,h)} + (\mu_h + h\xi_3)\mathrm{P}^{(t)}_{(s+1,k,h+1)} + \lambda_x b_1 \mathrm{P}^{(t)}_{(s-1,k,h)} + \lambda_y b_2 \mathrm{P}^{(t)}_{(s,k-1,h)} + \lambda_h b_3 \mathrm{P}^{(t)}_{(s,k,h-1)}$; $1 \le k \le s-1, 1 \le h \le s-1$
22. $\frac{dP^{(t)}_{(j,s,h)}}{dt} = -\big(\lambda_x b_1 + (\mu_x + (j-1)\xi_1) + (\mu_y + (s)\xi_2) + \lambda_h b_3 + (\mu_h + (h-1)\xi_3)\big)\mathrm{P}^{(t)}_{(j,s+1,h)} + (\mu_x(1-p_1) + j\xi_1)\mathrm{P}^{(t)}_{(j+1,s,h)} + (\mu_h + h\xi_3)\mathrm{P}^{(t)}_{(j,s,h+1)} + \lambda_x b_1 \mathrm{P}^{(t)}_{(j-1,s,h)} + \lambda_y b_2 \mathrm{P}^{(t)}_{(j,s,h)} + \lambda_h b_3 \mathrm{P}^{(t)}_{(j,s,h-1)}$; $1 \le j \le s-1, 1 \le h \le s-1$
23. $\frac{dP^{(t)}_{(j,k,s)}}{dt} = -\big(\lambda_x b_1 + (\mu_x + (j-1)\xi_1) + \lambda_y b_2 + (\mu_y + (k-1)\xi_2) + (\mu_h + (s-1)\xi_3)\big)\mathrm{P}^{(t)}_{(j,k,s)} + (\mu_x(1-p_1) + j\xi_1)\mathrm{P}^{(t)}_{(j+1,k,s)} + (\mu_y(1-p_2) + k\xi_2)\mathrm{P}^{(t)}_{(j,k+1,s)} + \lambda_x b_1 \mathrm{P}^{(t)}_{(j-1,k,s)} + \lambda_y b_2 \mathrm{P}^{(t)}_{(j,k-1,s)} + \lambda_h b_3 \mathrm{P}^{(t)}_{(j,k,s-1)}$; $1 \le j \le s-1, 1 \le k \le s-1$
24. $\frac{dP^{(t)}_{(s,s,s)}}{dt} = -\big((\mu_x + (s-1)\xi_1) + (\mu_y + (s-1)\xi_2) + (\mu_h + (s-1)\xi_3)\big)\mathrm{P}^{(t)}_{(s,s,s)} + \lambda_x b_1 \mathrm{P}^{(t)}_{(s-1,s,s)} + \lambda_y b_2 \mathrm{P}^{(t)}_{(s,s-1,s)} + \lambda_h b_3 \mathrm{P}^{(t)}_{(s,s,s-1)}$

Algorithm

1. Define the system parameters for Node-1, Node-2 and Central Server.
2. Represent arrival and service rates using triangular fuzzy, trapezoidal fuzzy, triangular intuitionistic fuzzy and trapezoidal intuitionistic fuzzy numbers.
3. Generate α-cut values for fuzzy models and β-cut values for intuitionistic fuzzy models.
4. Construct the finite state space X(t) = (N_1(t), N_2(t), N_3(t)), where 0 ≤ N_1, N_2, N_3 ≤ S
5. Construct the infinitesimal generator matrix Q by considering external arrivals, service completions, routing to the Central Server, balking and reneging.
6. Solve the transient probability equations dP(t)/dt = P(t)Q using the fourth-order Runge–Kutta method in MATLAB through
    - 6.1 Initialize the probability vector $p^{(0)}_{0,0,0}$=1 and step size h.
    - 6.2 Compute the RK4 coefficients:

$$k_1 = h(P_n Q), k_2 = h\left((P_n + \frac{k_1}{2})Q\right)$$
$$k_3 = h\left((P_n + \frac{k_2}{2})Q\right), k_4 = h((P_n + k_3)Q)$$

    - 6.3 Update the probability vector using: $P_{n+1} = P_n + \frac{1}{6}(k_1 + 2k_2 + 2k_3 + k_4)$
    - *6.4* Repeat Steps 2–3 for each time interval until the desired simulation time is reached, obtain the transient state probabilities.
7. At each time step, check that the total probability is approximately equal to one.
8. Compute expected system length for Node-1, Node-2 and Central Server using the transient state probabilities.
9. Compute the corresponding mean waiting times using the effective arrival rates.
10. Apply robust ranking and wingspan methods to obtain ranked performance measures.
11. Plot α-cut and β-cut based graphs for system length and waiting time.